Volume 21, No 2 | International Journal of Radiation Research, April 2023

Genome-wide profiling of DNA methylation and gene expression in radiation-resistant esophageal cancer cells

L-R Zhou[1,2,#], L. Wang[3,#], Z-C Tao[1,2,4,#], M. Cheng[5], J. Gao[1,2], L-T Qian[1,2*]

[1]Department of Radiation Oncology, The First Affiliated Hospital of USTC, Division of Life Sciences and Medicine, University of Science and Technology of China, Hefei, 230031, China
[2]Department of Radiation Oncology, Anhui Provincial Cancer Hospital, Hefei, 230031, China
[3]Department of Discipline Planning and Management, The First Affiliated Hospital of USTC, Hefei 230001, China
[4]School of Data Science, University of Science and Technology of China, Hefei, Anhui, 230026, China
[5]Laboratory of Molecular Oncology, Anhui Provincial Cancer Hospital, Hefei 230031, China

► ***Original article***

Corresponding author:
Dr. QIAN Li-ting
E-mail: *money2004@sina.com*

Received: March 2022
Final revised: September 2022
Accepted: November 2022

Int. J. Radiat. Res., April 2023; 21(2): 239-246

DOI: 10.52547/ijrr.21.2.9

Keywords: *Esophageal cancer cell line, Radiation tolerance, Gene microarray, DNA methylation.*

#These authors contributed equally to this work.

ABSTRACT

***Background*:** While there have been marked improvements in radiotherapeutic techniques in recent years, the emergence of radioresistance remains a pressing challenge to the clinical treatment of esophageal squamous cell carcinoma (ESCC). Altered DNA methylation is believed to play a role in the etiology of such resistance. This study was designed to explore patterns of altered genome-wide gene expression and DNA methylation patterns in radioresistant ESCC cells (TE1-res) in an effort to provide a foundation for the future study of the molecular drivers that underlie this form of therapeutic resistance. ***Materials and Methods*:** A microarray-based approach was used to conduct genome-wide DNA methylation and gene expression analyses using matched radioresistant and radioresistant ESCC cells. The mechanistic basis for ESCC cell radioresistance was then further examined through functional enrichment and protein-protein interaction analyses. ***Results*:** Relative to parental TE1 cells, TE1-res cells exhibited marked changes in their DNA methylation profiles, with the disproportional distribution of differentially methylated CpG sites (dmCpGs) in CpG islands and shore regions. Ontological analyses revealed that genes that were differentially expressed and methylated were enriched in the Ras protein signal transduction, regulation of DNA damage response, and angiogenesis pathways. Protein-protein interaction analyses further suggested that ACTL8, M-RAS, TRIB2, GATA5, ERBB4, FN1, DIRAS1, BTK, ROR1, and NPR3 may serve as hub proteins within TE1-res cells. ***Conclusions*:** These analyses revealed a significant association between DNA methylation and TE1-res cell radioresistance, highlighting several candidate genes and pathways that may be amenable to clinical targeting in an effort to increase the radiosensitivity of these ESCC cells.

INTRODUCTION

Esophageal carcinoma is among the most common causes of cancer-associated mortality in the world [(1)]. While radiotherapy is an integral component of therapeutic regimens for esophageal squamous cell carcinoma (ESCC) patients, the eventual emergence of radioresistant tumor cells can ultimately lead to locoregional recurrence, compromising efforts to effectively treat this disease. As such, there is a pressing need to better characterize the molecular mechanisms that govern the development of radioresistance.

DNA methylation is a heritable form of epigenetic modification resulting from the DNA methyltransferase-catalyzed addition of a methyl group to the fifth carbon of cytosine sites ($5^{me}C$) within the DNA [(2)]. Whereas mutations in the underlying genome are relatively rare, shifts in DNA methylation patterns are somewhat more common [(3)]. Cancer cells often exhibit the hypomethylation of specific promoter regions or the genome as a whole coupled with the hypermethylation of certain promoters. Promoters hypermethylation can suppress the expression of key tumor suppressor genes or other targets, whereas the global hypomethylation of transposable elements and repeated segments within the genome can contribute to increased chromosomal instability [(4)]. A correlation between increasing global genomic hypomethylation and more advanced tumor progression has been reported [(5)], and many studies have demonstrated that alterations in DNA methylation patterns play an important role in both normal physiology and oncogenic transformation [(6, 7)]. Abnormal DNA methylation also influences processes such as cellular adherence, toxic catabolic activity, the repair of DNA damage, angiogenesis, apoptosis, and cell cycle

[DOI: 10.52547/ijrr.21.2.9]

progression [8, 9]. Correlations between radiosensitivity and DNA methylation have also been detected in cultured cells [10, 11]. The processes of DNA methylation and demethylation are highly dynamic, with changes in these patterns occurring over minutes to hours in some cases [12]. Radiotherapy can induce changes in the DNA methylation profiles present within tumors, with these changes being closely associated with DNA damage response-related pathways [13]. Further research exploring the role of DNA methylation in the emergence of radioresistance may thus offer additional insights that can guide cancer patient treatment.

To facilitate the systematic analysis of the molecular drivers of radiation resistance in ESCC, our group previously generated a model of radioresistant ESCC cells (TE1-res) derived from the parental TE1 cell line through fractionated radiation exposure [14]. TE1-res cell proliferation was significantly enhanced, and these cells exhibited higher levels of radioresistance as compared to parental TE1 cells. Here, the HumanMethylation450 (HM450) BeadArray was used to identify genes that were differentially methylated between TE1-res and TE1 cells. This HM450 array includes coverage of 485,577 CpG sites, including 99% of genes annotated in RefSeq with several probes for each gene, including 96% of CpG islands (CGIs) annotated in the UCSC (The University of California Santa Cruz) database [15]. Through the combined analysis of microarray gene expression data and DNA methylation profiles, these analyses highlight a range of changes that may be important in the epigenetic control of ESCC cell radioresistance. The overall goal of this study is to offer additional insight regarding the importance of DNA methylation in the context of radiosensitivity. Of note, we observed several shifts in DNA methylation patterns in contrast to the negative correlations often reported between DNA hypermethylation and cancer -associated gene expression, offering a more detailed and nuanced view of these important regulatory processes.

MATERIALS AND METHODS

Cell culture

TE1 cells were obtained from the Cell Bank of the Chinese Academy of Sciences (Shanghai, China), and were cultured in RPMI-1640 (Invitrogen, USA) containing 10% fetal bovine serum (Invitrogen, USA) at 37°C in a humidified 5% CO_2 incubator. Culture medium was changed daily, and cells were passaged when confluent.

Radioresistant cell generation

TE1-res cells were generated as detailed in a prior report [14]. Briefly, TE-1 cell lines were cultured in 75 cm^2 flasks until 70-80% confluent, after they were washed twice with PBS, harvested using trypsin, and exposed to 2 Gy 6-MV X-ray irradiation (300 cGy/ min) with a CX-SN5340 instrument (VARIAN, America). After irradiation, culture medium was changed and cells were returned for routine culture. Cells were then subject to the same irradiation cycle when 70-80% confluent, with this process being repeated 8 times for a total dose of 16 Gy.

Clonogenic survival assay

To identify radioresistant TE1 cells, cells were added to 6-well plates and subjected to X-ray irradiation (0, 2, 4, 6, 8, or 10 Gy) at room temperature. Cells were then cultured for 14 days during which colonies were allowed to grow. Crystal violet was then used to stain colonies, and colonies containing more than 50 cells were counted. Analyses were repeated in triplicate, and the surviving fraction (SF) was calculated by dividing the number of surviving colonies by the number of cells seeded upon initial plating.

Apoptosis analyses

An Annexin V-FITC Apoptosis Detection Kit (BD Biosciences, CA, USA) and 7-AAD (BD Biosciences) were used based on provided directions to detect apoptotic cell death. Briefly, cells were cultured and irradiated as above in 75 cm^2 flasks, after which they were harvested, rinsed using PBS, and resuspended for 10 min in binding buffer containing Annexin V and 7-AAD on ice while protected from light. Samples were then analyzed with a FACS Calibur flow cytometer (BD Biosciences).

Infinium humanmethylation450 beadArray

After bisulfite conversion, DNA was used with an Infinium HumanMethylation450 BeadArray (Illumina, Inc.) to detect methylation patterns. Methylation levels at individual CpG sites were represented by β-values, which are continuous variables ranging from 0 (complete demethylation) to 1.0 (complete methylation). A given CpG site was considered hypermethylated or hypomethylated in the measured Δβ values when comparing TE1 and TE1-res cells were > 0.2 or < -0.2, respectively.

Human v5 expression beadchip

Total RNA extracted from TE1 and TE1-res cells was analyzed with the Human v5 Expression BeadChip (Illumina, Inc.) based on provided directions. This chip includes 175,906 probes spanning ~40,000 genes. Differential gene expression was established based on a P-value < 0.05 and a fold change (FC) less than 0.5 or greater than 2.

Gene ontology (GO) analyses

As promoter methylation often suppresses gene expression, we next cross-referenced differentially

[DOI: 10.52547/ijrr.21.2.9]

expressed genes in TE1-res cells with methylation data. In total, 3251 genes were separated into those that were significantly up- or down-regulated (|log2 fold change| > 1), while DNA methylation data were filtered to only focus on probes in promoter regions exhibiting a significant change in methylation (|Δβ| > 0.2). A total of 1304 hypermethylated, downregulated genes and 887 hypomethylated, upregulated genes were then retained and analyzed with the agriGO tool using default parameters for Fisher's t-test (P<0.05).

Protein-protein interaction (PPI) analyses

The 300 most significantly regulated genes identified when comparing TE1-res and TE1 cells were subject to PPI analyses performed with the Search Tool for the Retrieval of Interacting Genes/ Proteins database (String-DB), with network visualization being achieved using Cytoscape v 3.2.1 [16]. The connection strength (degree) values for all nodes within the PPI network were determined [17] and hub nodes with high connectivity values were posited to play central roles in the process of radioresistance. Hub proteins were defined as those in the top 5% of the degree value distribution.

Real-time polymerase chain reaction (RT-PCR) analyses

TRIzol (Invitrogen, USA) was used based on provided directions to extract total RNA from TE1 and TE1-res cells, after which RT-PCR analyses of these RNA samples were performed using 1 μl of cDNA, 10 μl of SYBR Premix ExTaq (Takara, Japan), and 2 μl of appropriate primers (table 1) using a LightCycler instrument (Roche Diagnostics, Germany). Three genes differentially expressed between TE1 and TE1-res cells (TFPI-2, DLC1, and PRDM16) were selected at random for analysis, while β-actin served as a normalization control. Samples were analyzed in triplicate, and relative expression was measured using the 2ΔΔCt method. Data are given as means ± SEM, and P<0.05 was the significance threshold.

Table 1. Primers sequences using in RT-PCR.

Gene symbol	Forward(5'-3')	Reverse(5'-3')
TFPI-2	GGGCCCTACTTCTCCG TTAC	CACAC-TGGTCGTCCACACTC
DLC1	CCGCCTGAG-CATCTACGA	TTCTCCGACCAC-TGATTGACTA
PRDM16	AGTGAGATGAACCAA-GCATCAACG	CTGCACAGTG-TATGTTTTAAAGCC

Bisulfite sequencing PCR

A Qiagen DNAeasy Kit (Qiagen, CA, USA) was used to extract total DNA from cell suspensions based on provided directions, after which pyrosequencing DNA (5 μg/cell line) was subject to bisulfite treatment with the Zymo EZ DNA Methylation Lightning kit (Zymo Cat. No.D5030). Appropriate primers designed with Methyprimer 11.0 (see table 2) were then used to amplify this bisulfite-modified DNA via PCR. Individual PCR reactions consisted of 1x PCR buffer and 50 ng of bisulfite-modified DNA in a total volume of 25 μL. Reactions were initially incubated for 3 min at 94°C, followed by the addition of 1.5 U of Taq DNA polymerase (Roche Diagnostic GmbH, Mannheim, Germany). Amplification was then performed with the following settings: 45 cycles of 90°C for 30 s, 56°C for 30 s, and 72°C for 50 s; 72 °C for 5 min. All analyses were repeated a minimum of two times with sets of DNA that had been independently subject to bisulfite modification.

Table 2. Primers sequences using in BSP.

Gene symbol	P1(5'-3')	P2(5'-3')
SPINT2	AATTTCCAC-CTCTGAGGCTTGAATG	CCTTCTGGAAGGGACAC-TTTGCTAA
CDKN1B	CAGCCAGAGCAGGTTT-GTTGGCAGT	CCTCCTCTGTTTAAA-TAGACTTGCA
DKK1	AGGGTCCCTGAA-GCCTGGTCAGTCCT	GACAGGAGGAA-TAACCCTCTAGGGA
TP53	CCCCTTGTTGAA-GCTCCTGGGACACA	GGCCAGGTCAG-GAGGGAGGCTATC
PPP2R1B	GATGAATCCCTGCCCTT-GTTTCTTT	GACCAGCCAGAGGAGGAA-GAACATGG

RESULTS

Identification of differentially methylated genes in TE1-res cells

To examine the potential role that epigenetic changes play in the development of tumor cell radioresistance, the HM450 BeadArray was used to conduct genome-wide analyses of DNA methylation status in TE1-res and TE1 cells. Of the ~100,000 probes included on this chip that were differentially methylated in TE1-res cells, 46,883 and 58,024 were hypermethylated and hypomethylated, respectively (figure. 1A). Both cell lines exhibited similar bimodal β-value distributions (figure 1B-C). In line with prior evidence[18], two peaks were observed corresponding to CpG sites that were highly methylated and those that were less methylated. A slightly lower proportion of hypermethylated CpG sites was evident in TE1-res cells relative to TE1 cells (45.66% vs 49.32% for CpG sites with a β-value > 0.8). For further details regarding methylation β-values for all CpG sites, see figure 1D.

Analyses of differentially methylated CpG site distributions

Next, a computational analysis was used to explore differences in differentially methylated CpG sites distributions in radioresistant cells based on the results of these HM450 BeadArray analyses. The locations of these CpG sites are summarized in figures 2A and B. Roughly 34% of the sites that were hypermethylated in TE1-res cells were located in

[DOI: 10.52547/ijrr.21.2.9]

open sea regions, with fewer in shore (31.04%), CpG island (28.37%), and shelf (15.85%) regions (figure 2A). Hypomethylated CpG sites were located in open sea (45.91%), shore (22.53%), island (19.12%), and shelf (12.44%) regions (Fig. 2B). Changes in CpG levels between these two cell lines were evident in both canonical CpG islands as well as in shore and open sea areas.

As dmCpGs in CpG island regions are more frequently considered to play a role in the epigenetic control of gene expression[3], those dmCpGs present within islands in this study were further analyzed to establish their functional genomic distributions. Hypermethylated CpG sites in island regions were more often located within gene promoters (30.92%), while hypomethylated CpG sites in CpG island regions were relatively evenly distributed across promoter (25.94%), gene body (27.66%), and intergenic regions (25.43%) (figure 2C-D).

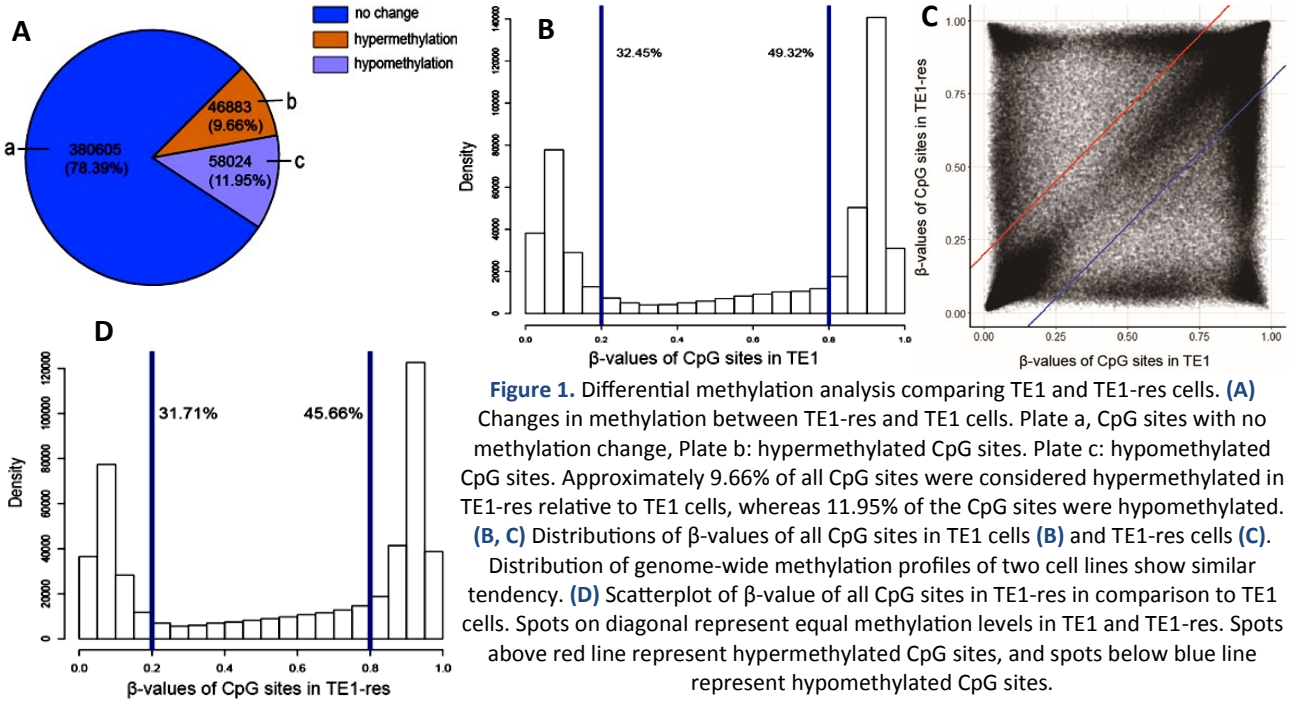

Figure 1. Differential methylation analysis comparing TE1 and TE1-res cells. **(A)** Changes in methylation between TE1-res and TE1 cells. Plate a, CpG sites with no methylation change, Plate b: hypermethylated CpG sites. Plate c: hypomethylated CpG sites. Approximately 9.66% of all CpG sites were considered hypermethylated in TE1-res relative to TE1 cells, whereas 11.95% of the CpG sites were hypomethylated. **(B, C)** Distributions of β-values of all CpG sites in TE1 cells **(B)** and TE1-res cells **(C)**. Distribution of genome-wide methylation profiles of two cell lines show similar tendency. **(D)** Scatterplot of β-value of all CpG sites in TE1-res in comparison to TE1 cells. Spots on diagonal represent equal methylation levels in TE1 and TE1-res. Spots above red line represent hypermethylated CpG sites, and spots below blue line represent hypomethylated CpG sites.

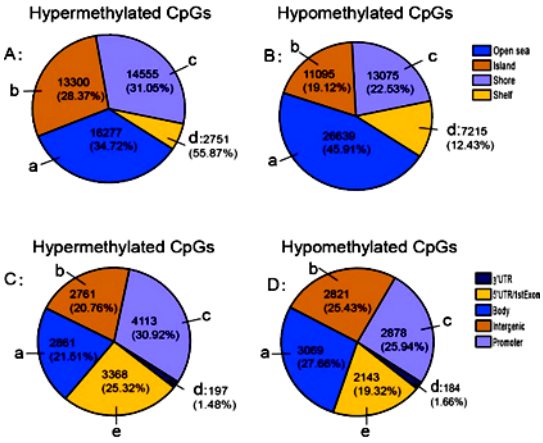

Figure 2. Disproportional distributions of CpG sites. **(A, B)** Neighborhood relationship between dmCpG sites and CpG islands in TE1-res cells. **(A)** represents hypermethylated CpG sites, and **(B)** denotes hypomethylated CpG sites in TE1-res cells, dmCpG sites are distributed in CpG islands(Plate b), shores (regions up to 2 kb from CGIs, Plate c), shelves (2 to 4 kb from CGIs, Plate d) and open sea regions(Plate a). **(C, D)** Genomic distributions of hypermethylated CpG sites **(C)** and hypomethylated CpG sites **(D)** in islands. Hypermethylated CpG sites in islands occurred more often in promoter regions (Plate c), whereas hypomethylated CpG sites were distributed equally among promoters, gene body (Plate a), intergenic (Plate b) and gene -regulatory regions, including 3' UTR (Plate d),5' UTR/1stExon (Plate e).

GO enrichment analyses highlight radioresistance-related pathways

To more fully understand the potential functional implications of genes that were differentially expressed and methylated when comparing TE1-res and TE1 cells, GO enrichment analyses were next performed. This approach highlighted multiple significantly enriched biological processes ($P < 0.01$), offering a gene list associated with the acquisition of radiation resistance in these cells (table 3). Genes that were hypermethylated and downregulated were associated with the Ras/P53 pathways, while genes that were hypomethylated and upregulated genes were enriched in the wound healing, cell-cell signaling, and regulation of angiogenesis pathways.

PPI analyses highlight hub proteins that may govern the function of radioresistant ESCC cells

A BeadChip gene expression analysis revealed significant changes in the expression of 11,458 probes in TE1-res cells relative to TE1 cells (figure 3A). The 10 most strongly up- and down-regulated genes were

[DOI: 10.52547/ijrr.21.2.9]

identified as potential regulators of radioresistance (table 4).

Table 3. GO analysis for differentially methylated and expressed genes.

GO term	P-value	Gene symbol
Hypermethylated-down expression genes		
Negative Regulation of cell migration	0.00076	AB-HD6;ACVR1C;ADARB1;APOE;ARHGAP4;ARHGDIB;BCR;BRAF;BST2;CHRD;DACH1;DPYSL3;FUZ;ITGB1BP1;PADI2;PDGFB;PLCB1;PTPRM;RABGEF1;RNF41;STAT3;TIMP1;TP53INP1;VASH1
Ras protein signal transduction	0.0070	AP-OE;ARHGAP29;ARHGAP4;ARHGDIB;ARHGEF1;ARHGEF2;ARRB1;CDKN2A;COL1A2;CTNNAL1;DBNL;EPS8L1;F2R;ITGA3;ITPKB;MAP-K13;MRAS;RAB12;RAB15;RAB24;RAB27A;RAB31;RAB36;RAB42;RAB4B;RABGEF1;RASAL2;RASGRF1;TIAM1;TIMP2;VANGL2
regulation of DNA damage response, signal transduction by p53 class mediator	0.0070	CD74;CDKN2A;KDM1A;PLA2R1;SENP2;SPRED2
Hypomethylated-up expression genes		
Wound healing	0.000007	ANGPT1;ANGPT4;ANXA2;APCS;ATP2B2;ATP2B3;CABLES1;CAV1;CCL20;CD40LG;CD48;CLEC4M;DGKD;DSP;ERBB4;F12;F13A1;FGF2;FN1;FOXA2;GATA6;GP1BA;HIF1A;HIST1H3F;HIST1H3I;HIST1H3J;HOPX;HRAS;IL24;INPP5D;INS;ITGAM;KCNMB1;KLC2;LARGE;LEFTY2;LOX;MRVI1;MYOD1;OLR1;PECAM1;PIK3R6;PLAT;PLAU;POU2F3;SAA1;SCAR-A5;SELP;SLC11A1;SLC7A8;SPARC;SPN;TFPI;THPO;TREM1;VEGFC;VWF;WAS
Cell adhesion	0.00004	ACT-N3;ADAM12;ANGPT1;AZGP1;BCL10;BCL11A;BCL11B;BOC;CASP3;CAV1;CCDC80;CCL5;CD209;CD300A;CD3E;CD40LG;CD7;CD80;CDH22;CLDN6;CLEC4M;COL28A1;COL4A6;CSTA;CTLA4;DLL1;DSG2;DSP;DUSP26;EDIL3;EFNB1;FAM21C;FAP;FAT2;FERMT2;FEZ1;FLRT2;FN1;FOXA2;GCNT2;GP1BA;HAPLN2;HEPACAM;HHLA2;HLA-DOA;HOXA7;HSD17B12;IDO1;IGFBP7;IL1RN;IL27;IL32;INS;ITGA11;ITGAM;LIMS1;LY6D;LY9;MEGF11;MLLT4;MTSS1;MYBPC3;MYBPH;NCK2;NPHS1;OLR1;OTOA;PARVG;PE-CAM1;PLAU;PPP2CA;PVRL3;RELN;RNASE10;SAA1;SELP;SIGLEC11;SIGLEC8;SIGLEC9;SLA2;SLC11A1;SMAD6;SPN;SVEP1;TBCD;THBS2;TNN;TREML2;VEGFC;VWA2;VWF;WAS;ZBTB32
cell-cell signaling	0.00038	ADCY2;AP3M2;ATP2B2;BTK;CACNA1B;CACNG3;CACNG4;CCL16;CCL20;CCL5;CD70;CD80;CHAT;CHRM4;CHRNA6;CHRNB3;CPLX2;CPT1A;CRHR1;CSPG5;CYB5R4;DBN1;DLL1;DTNA;EFNB1;FADS1;FFAR2;FGFR4;FOXA2;GABRA1;GAD2;GJB2;GNB3;GPR119;GRIK5;GRIN2A;HCRTR1;HIF1A;HMGA2;HNF1A;HRAS;HRH3;IL1RN;INS;KCNG4;KCNK9;KCNMB1;KCNQ5;KCNS2;LPAR3;MLLT4;MTMR2;NEFL;NR0B2;NR2E1;OPRD1;OXT;P2RX2;PCSK1;PCSK5;PLAT;PPY;PTPRN;RAPSN;RELN;SERPINB3;SHANK1;SIX1;SIX3;SLC12A5;SLC17A7;SMPD3;SNCAIP;SREBF1;SSTR3;SSTR5;STAR;SYT6;TMEM27;TP63
regulation of angiogenesis	0.0069	AMOT;ANGPT4;C3AR1;CRHR2;ENPP2;FGF2;GATA6;HIF1A;KLK3;MMRN2;NPPB;NR2E1;OPTC;PIK3R6;SPARC;THBS2;VEGFC

Table 4. The 10 most strongly up- and down-regulated genes.

Gene Symbol	Fold change	Gene Symbol	Fold change
FAT2	57545.00161	XLOC_l2_001359	0.000112813
MAGEA6	3344.882924	XLOC_013218	0.000208683
NR2F2	1736.918565	MGST1	0.000210123
KRT5	1587.771621	IGF2	0.000214599
FAM178A	1466.205899	EEF1A2	0.000376554
DDX43	694.5066991	ICAM2	0.000590455
C9orf125	531.4157955	C8orf31	0.000647322
AKAP17A	500.7725249	TUSC3	0.000671951
CXCR7	422.6139267	BST2	0.00075688
ARFIP1	420.2645623	MEST	0.00087894

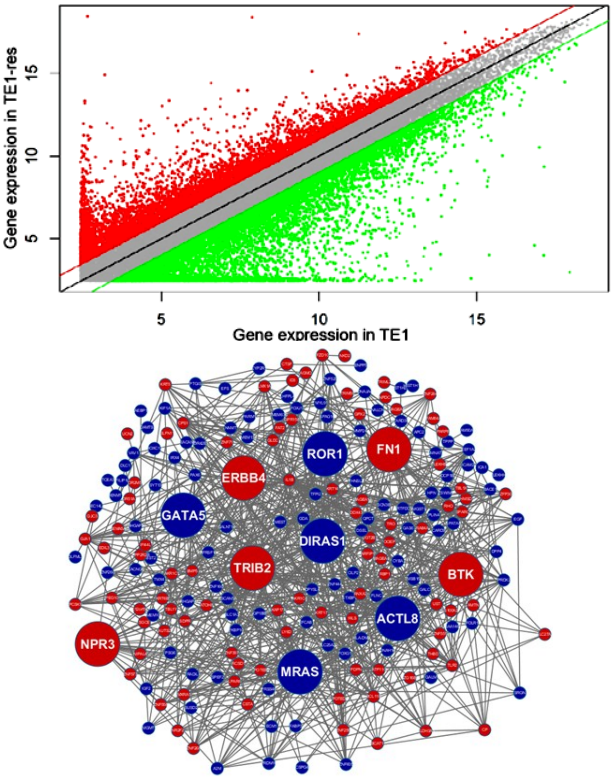

Figure 3. Genome-wide gene expression analysis. **(A)** Scatterplot of all probes between TE1 and TE1-res cells. Spots above or below diagonal denote differentially expressed genes in gene array. **(B)** Protein-protein interactions of 300 most significantly regulated genes.

To explore the mechanisms that underlie the acquisition of such resistance, PPI analyses were performed for the 300 most significantly regulated proteins, leading to the construction of a PPI network comprised of 209 nodes and 817 edges (figure. 3B). In this network, 10 nodes (ACTL8, M-RAS, TRIB2, GATA5, ERBB4, FN1, DIRAS1, BTK, ROR1, and NPR3) were identified as hub proteins that may play a role in mediating TE1-res radioresistance owing to their high levels of connectivity (table 5).

RT-PCR-based validation of differential gene expression data

To validate the above BeadChip gene expression

[DOI: 10.52547/ijrr.21.2.9]

analysis results, three genes were randomly selected for RT-PCR analysis. The observed DLC1, TFPI-2, and PRDM16 expression levels in TE1-res cells were significantly decreased relative to TE1 cells (P-values: 7.10436E-05, 1.18128E-10, and 3.44157E-10, respectively), consistent with the results from the BeadChip analysis (Respective FC values of 0.0048, 0.001, and 0.004) (figure 4).

Table 5. Hub proteins in PPIs.

Gene symbol	degree	fold-change	Δβ
ACTL8	38	0.0018	0.38
MRAS	33	0.01	0.37
TRIB2	31	52.85	-0.92
GATA5	31	0.0032	0.39
ERBB4	31	74.30	-0.60
FN1	31	72.73	-0.50
DIRAS1	30	0.0055	0.34
BTK	29	42.62	-0.85
ROR1	28	0.0061	0.24
NPR3	27	67.47	-0.63

Note: Δβindicates the average value of methylation change between TE1 and TE1-res cells.

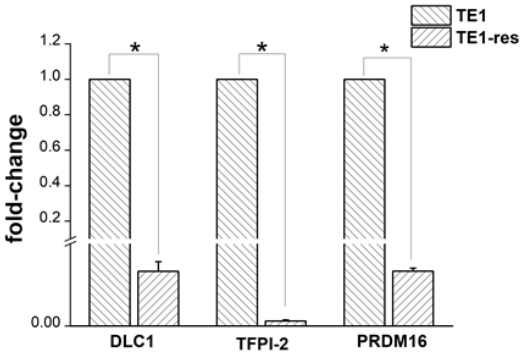

Figure 4. Verification of gene expressions by qPCR. Up-regulated genes DLC1, TFPI-2, and PRDM16 in TE1-res cell line were detected by qPCR.

DISCUSSION

In this study, HumanMethylation 450K arrays were used to conduct genome-wide analyses of changes in DNA methylation associated with the acquisition of radioresistance in ESCC cells. CpG islands harbor the transcriptional start sites for ~60% of human genes that encode proteins [19], and the methylation of these island regions can readily suppress transcriptional activity even though they comprise just ~1% of the human genome [20]. CpG island shores, which consist of the 2 kb regions flanking these islands are also associated with altered gene expression, as are the further 2 kb flanking regions known as CpG island shelves [16]. The present results are consistent with those published by Ogoshi *et al.* [15] and Irizarry *et al.* [21], who observed that colon cancer cells exhibit the differential methylation of many sites, the majority of which were located in intergenic and CpG island shore regions. CpG Island shores have been shown to exhibit the highest levels of variability in DNA methylation [22], and the cancer-specific methylation of these regions is related to altered transcriptional activity. These data suggest that a wide array of DNA methylation-related mechanisms play a role in governing radiotherapy-associated responses to DNA damage.

In the present analyses, dmCpGs were found to be located in promoter-associated CpG islands as well in intergenic, gene body, and 5'-UTR/1st exon regions. Prior work[23] has demonstrated that changes in DNA methylation in three non-promoter regions in breast cancer were linked to increased gene expression, emphasizing the relevance of DNA methylation changes at multiple sites throughout the genome in the context of invasive breast cancer. Another recent research effort examined DNA methylation profiles in primary colorectal tumors and liver metastases [24], leading to the detection of higher levels of hypermethylated dmCpGs in intragenic, gene-regulatory regions, while dmCpGs that were hypomethylated were largely evenly distributed across promoters, intergenic (primarily open sea) regions, and intragenic (primarily gene body) regions, in line with our results. CpG islands located in intragenic regions that control genomic elements and gene expression may thus function as regulators of TE1-res cell radioresistance. Over 50% of all CpG islands in the human genome are located in intragenic regions and between coding regions. Roughly 42% of the orphan CpG islands not located proximal to annotated promoter regions are associated with transcriptional initiation sites [20], and these may correspond to promoters for non-annotated genes or non-coding RNAs [25]. Prior studies [26] have also revealed that high levels of methylation are evident throughout the gene bodywith these levels sharply decreasing and increasing across exon-intron junctions and at sites of transcriptional termination. Accordingly, we hypothesized that changes in the DNA methylation status of intragenic regions have the potential to contribute to the emergence of radioresistance-related shifts in gene expression through the preferential utilization of alternative promoters and the altered splicing of associated mRNAs [27, 28]. To test this model, further studies focused on areas other than the promoter region are warranted to clarify the relationship between radioresistance and CpG island methylation.

GO annotation analyses suggest that the altered regulation of multiple signaling pathways as a consequence of changes in DNA methylation may play a role in the emergence of radioresistant phenotypes. As such, the annotated genes associated with these pathways may represent viable targets for radiosensitization-focused clinical intervention. However, additional research will be critical in order to clarify whether changes in the methylation of any individual gene identified in this study can ultimately

[DOI: 10.52547/ijrr.21.2.9]

translate to a change in cellular radiosensitivity.

PPI networks offer a powerful approach to exploring complex relationships among different proteins such that key regulators of these dynamic interactions can be selected for further analysis. Of the hub proteins identified in this study, TRIB2 was the most extensively hypomethylated in radioresistant ESCC cells, and it has also been shown to function as an oncogene capable of interacting with E3 ubiquitin ligases in AML [29], glioblastoma [30], liver [31], and colorectal cancer [32]. Owing to its ability to modulate a range of transcription factors and signaling molecules, TRIB2 occupied a central role in the developed PPI network. Mechanistically, TRIP2 may drive oncogenic progression through the Hippo/YAP and C/EBPα-involved pathways. C/EBPα (CCAAT enhancer binding protein α) is a myeloid transcription factor that can suppress tumor development, induce cell cycle arrest, and drive differentiation towards the granulocytic lineage [33]. TRIB2 can promote the degradation of C/EBPα p42 [34]. TRIB2 can additionally stabilize Yes-associated protein (YAP) stabilization and transactivation degradation by interacting with the βTrCP ubiquitin ligase [35], with the terminal effector protein YAP serving to promote oncogenesis. As such, TRIB2 can play dual roles as a negative or positive regulator of proteasomal degradation. TRIB2 has also recently been reported to function in the context of tumor cell drug resistance [36]. No prior studies have examined changes in TRIB2 methylation and expression in ESCC. In this study, we observed profound TRIB2 hypomethylation ($\Delta\beta < -0.9$) in TE1-res cells, with a corresponding ~50-fold increase in the expression of this gene relative to TE1 parental cells. Whether DNA methylation controls the expression of TRIB2 in this context remains to be formally tested. However, as this protein is a central regulator of tumorigenic processes and it can influence the expression and activity of important proteins associated with cell cycle arrest, it may represent a promising target associated with tumor cell radioresistance.

In summary, we herein compared patterns of DNA methylation and gene expression between radioresistant and parental radiosensitive ESCC cells in an effort to shine a light on the epigenetic control of radioresistance. We found that dmCpGs located in shore and gene body regions may play an important role in shaping the process of radioresistance, as may dmCpGs in CpG island regions. GO analyses suggested that these changes in DNA methylation and gene expression are associated with the induction of responses mediated through pathways that can protect cells against ionizing radiation. The acquisition of radiation resistance may be in part associated with TRIB2 upregulation. However, further in-depth research focused on the specific proteins and pathways that govern this process will be essential to more fully clarify how epigenetic processes regulate ESCC cell radiosensitivity.

ACKNOWLEDGEMENTS

We would like to thank Bai Lu for her preliminary work on this research.

***Ethical consideration*:** Declared none.

***Funding*:** This research was funded by "Hefei City, Science and Technology Bureau Foundation (J2020Y01)".

***Conflicts of interest*:** Declared none.

***Author contributions*:** Data curation: ZHOU Ling-ran, WANG Liang, Data analyses: ZHOU Ling-ran, TAO Zhen-chao, Funding acquisition: QIAN Li-ting, Manuscript revision: GAO Jin, Study design: CHENG Min, QIAN Li-ting, and Writing - original draft: ZHOU Ling-ran, WANG Liang.

REFERENCES

1. Sung H, Ferlay J, Siegel RL, Laversanne M, Soerjomataram I, Jemal A, *et al.* (2021) Global Cancer Statistics 2020: GLOBOCAN Estimates of Incidence and Mortality Worldwide for 36 Cancers in 185 Countries. *CA Cancer J Clin*, **71**(3): 209-249.
2. Zielske SP (2015) Epigenetic DNA methylation in radiation biology: on the field or on the sidelines? *J Cell Biochem*, ***116****(2): 212-217*.
3. You JS and Jones PA (2012) Cancer genetics and epigenetics: two sides of the same coin? *Cancer Cell*, ***22****(1): 9-20*.
4. Ambrosi C, Manzo M, Baubec T (2017) Dynamics and Context-Dependent Roles of DNA Methylation. *J Mol Biol*, ***429****(10): 1459-1475*.
5. Ehrlich M (2009) DNA hypomethylation in cancer cells. *Epigenomics*, ***1****(2): 239-259*.
6. Szigeti KA, Galamb O, Kalmar A, Bartak BK, *et al.* (2018) Role and alterations of DNA methylation during the aging and cancer. *Orv Hetil*, ***159****(1): 3-15*.
7. Mangelinck A and Mann C (2021) DNA methylation and histone variants in aging and cancer. *Int Rev Cell Mol Biol*, ***364****: 1-110*.
8. Simo-Riudalbas L and Esteller M (2014) Cancer genomics identifies disrupted epigenetic genes. *Hum Genet*, ***133****(6): 713-725*.
9. Raiche J, Rodriguez-Juarez R, *et al.* (2004) Sex- and tissue-specific expression of maintenance and de novo DNA methyltransferases upon low dose X-irradiation in mice. *Biochem Biophys Res Commun*, ***325****(1): 39-47*.
10. Miousse IR, Kutanzi KR, Koturbash I (2017) Effects of ionizing radiation on DNA methylation: from experimental biology to clinical applications. *Int J Radiat Biol*, ***93****(5): 457-469*.
11. Chen X, Liu L, Mims J, Punska EC, *et al.* (2015) Analysis of DNA methylation and gene expression in radiation-resistant head and neck tumors. *Epigenetics*, ***10****(6): 545-561*.
12. Newman MR, Sykes PJ, Blyth BJ, *et al.* (2014) The methylation of DNA repeat elements is sex-dependent and temporally different in response to X radiation in radiosensitive and radioresistant mouse strains. *Radiat Res*, ***181****(1): 65-75*.
13. Antwih DA, Gabbara KM, Lancaster WD, *et al.* (2013) Radiation-induced epigenetic DNA methylation modification of radiation-response pathways. *Epigenetics*, ***8****(8): 839-848*.
14. Lu B, Liang W, Lingran Z, Min C, Liting Q (2016) Cancer stem cells in radiation resistance of esophageal cancer: role and molecular mechanism. *Chinese Journal of Radiation Oncology*, ***25****(4): 401-406*.
15. Ogoshi K, Hashimoto S, Nakatani Y, *et al.* (2011) Genome-wide profiling of DNA methylation in human cancer cells. *Genomics*, ***98*** *(4): 280-287*.
16. Shannon P, Markiel A, Ozier O, *et al.* (2003) Cytoscape: a software environment for integrated models of biomolecular interaction networks. *Genome Res*, ***13****(11): 2498-2504*.
17. Yu H, Kim PM, Sprecher E, Trifonov V, Gerstein M (2007) The importance of bottlenecks in protein networks: correlation with gene essentiality and expression dynamics. *PLoS Comput Biol*, ***3****(4): e59*.

[DOI: 10.52547/ijrr.21.2.9]

18. Kim EH, Park AK, Dong SM, Ahn JH, Park WY (2010) Global analysis of CpG methylation reveals epigenetic control of the radiosensitivity in lung cancer cell lines. *Oncogene*, ***29****(33): 4725-4731*.
19. Saxonov S, Berg P, Brutlag DL (2006) A genome-wide analysis of CpG dinucleotides in the human genome distinguishes two distinct classes of promoters. *Proc Natl Acad Sci U S A*, ***103****(5): 1412-1417*.
20. Illingworth RS, Gruenewald-Schneider U, Webb S, *et al.* (2010) Orphan CpG islands identify numerous conserved promoters in the mammalian genome. *PLoS Genet*, ***6****(9): e1001134*.
21. Irizarry RA, Ladd-Acosta C, Wen B, Wu Z, *et al.* (2009) The human colon cancer methylome shows similar hypo- and hypermethylation at conserved tissue-specific CpG island shores. *Nat Genet*, ***41*** *(2): 178-186*.
22. Ji H, Ehrlich LI, Seita J, Murakami P, *et al.* (2010) Comprehensive methylome map of lineage commitment from haematopoietic progenitors. *Nature*, ***467****(7313): 338-342*.
23. Rao X, Evans J, Chae H, Pilrose J, *et al.* (2013) CpG island shore methylation regulates caveolin-1 expression in breast cancer. *Oncogene*, ***32****(38): 4519-4528*.
24. Orjuela S, Menigatti M, Schraml P, *et al.* (2020) The DNA hypermethylation phenotype of colorectal cancer liver metastases resembles that of the primary colorectal cancers. *BMC Cancer*, ***20****(1): 290*.
25. Medvedeva YA, Fridman MV, Oparina NJ, *et al.* (2010) Intergenic, gene terminal, and intragenic CpG islands in the human genome. *BMC Genomics*, **11**: 48.
26. Lister R, Pelizzola M, Dowen RH, *et al.* (2009) Human DNA methylomes at base resolution show widespread epigenomic differences. *Nature*, ***462****(7271): 315–322*.
27. Yang X, Han H, Carvalho DDD, *et al.* (2014) Gene Body Methylation can alter Gene Expression and is a Therapeutic Target in Cancer. *Cancer Cell*, ***26****: 577–590*.
28. Maunakea AK, Nagarajan RP, Bilenky M, *et al.* (2010) Conserved role of intragenic DNA methylation in regulating alternative promoters. *Nature*, ***466****(7303): 253-257*.
29. O'Connor C, Yalla K, Salome M, *et al.* (2018) Trib2 expression in granulocyte-monocyte progenitors drives a highly drug resistant acute myeloid leukaemia linked to elevated Bcl2. *Oncotarget*, ***9*** *(19): 14977-14992*.
30. Wang J, Zuo J, Wahafu A, Wang MD, *et al.* (2020) Combined elevation of TRIB2 and MAP3K1 indicates poor prognosis and chemoresistance to temozolomide in glioblastoma. *CNS Neurosci Ther*, ***26*** *(3): 297-308*.
31. Guo S, Chen Y, Yang Y, Zhang X, *et al.* (2021) TRIB2 modulates proteasome function to reduce ubiquitin stability and protect liver cancer cells against oxidative stress. *Cell Death Dis*, ***12****(1): 42*.
32. Hou Z, Guo K, Sun X, Hu F, Chen Q, Luo X, *et al.* (2018) TRIB2 functions as novel oncogene in colorectal cancer by blocking cellular senescence through AP4/p21 signaling. *Mol Cancer*, ***17****(1): 172*.
33. Porse BT, Bryder D, Theilgaard-Monch K, *et al.* (2005) Loss of C/EBP alpha cell cycle control increases myeloid progenitor proliferation and transforms the neutrophil granulocyte lineage. *J Exp Med*, ***202****(1): 85-96*.
34. Dedhia PH, Keeshan K, Uljon S, Xu L, *et al.* (2010) Differential ability of Tribbles family members to promote degradation of C/EBPalpha and induce acute myelogenous leukemia. *Blood*, ***116****(8): 1321-1328*.
35. Wang J, Park JS, Wei Y, Rajurkar M, *et al.* (2013) TRIB2 acts downstream of Wnt/TCF in liver cancer cells to regulate YAP and C/EBPalpha function. *Mol Cell*, **51**(2): 211-225.
36. Machado S, Silva A, De Sousa-Coelho AL, *et al.* (2020) Harmine and Piperlongumine Revert TRIB2-Mediated Drug Resistance. *Cancers (Basel)*, **12**(12).

[DOI: 10.52547/ijrr.21.2.9]